

Image Fusion of 3D MR-Images to improve the spatial resolution

C. Vogelbusch¹, S. Henn², J.K. Mai³, T. Voss³ und K. Witsch¹

¹Mathematisches Institut, Lehrstuhl für Angewandte Mathematik,
Heinrich-Heine-Universität Düsseldorf, Germany

²Mathematisches Institut, Lehrstuhl für Mathematische Optimierung,
Heinrich-Heine-Universität Düsseldorf, Germany

³Institut Anatomie I, Heinrich-Heine-Universität Düsseldorf, Germany
eMail:Christoph@VogelbuschNet.de

Abstract. In this paper we present an approach to combine the information of n MR images the so-called source images $\{S_i\}_{1 \leq i \leq n}$ – monitored from different directions – into a so-called fused image I which should include the features of each source image. The so-called image fusion process cuts into two steps. First an affine linear mapping is determined, so that the so-called sum of squared differences, between the source images is as small as possible. Furthermore, a trilinear interpolation is used to combine the information of the matched source images. The image fusion approach is tested on real MR images provided by the Institute of Anatomie I, Heinrich-Heine-Universität Düsseldorf.

1 Introduction

The resolution of MR images has been steadily increased during the past years. However, it is still very limited with respect to the underlying histology. The resolution obtained in clinical settings is normally in the range of one square-millimeter; the magnification at which the structural information is derived by light microscopy is higher by a factor of between 100 and 1000. This means that the correlation between morphological and functional information is far from optimum.

Our goal is to narrow the gap in resolution between clinical MR images and underlying tissue. The imaging modalities providing the highest resolution, however, obtain this only in two but not in three dimensions greatly affecting 3-dimensional reconstruction. In order to compensate for the loss of detail we developed a image fusion approach which renders an increased resolution throughout tissue volume. Image fusion is a way of combining information of several images given e.g. by different spatial resolution or different sensors. The result is a product that synergistically combines the best features of each of its components. In this paper we provide a powerful image fusion approach to combine MR images together.

In our situation n 3D-MR source images $\{S_i\}_{1 \leq i \leq n}$ from a single object, recorded in frontal, sagittal and/or horizontal direction are given. Each set consist of a moderate number of slides (e.g. 70-100) with high resolution (e.g.

512×512). The aim of the proposed image-fusion approach is to incorporate information of the images to one fused image I with highest resolution (e.g. $512 \times 512 \times 512$), so that the details of the images are well preserved.

2 Image fusion of MR images

In the following the image fusion approach is illustrated for several MR images monitored from different directions. The MR images are recorded in the DICOM format. We start the image fusion process by an affine linear matching of the images. Within the matching process the reference image is defined w.l.o.g. by the first source image S_1 . The optimal transformations are determined by minimizing the sum of squared differences

$$g(A, b) = \|S_1 - S_i(f^{(i)}(A, b))\|_2^2 \quad \text{for } i = 2, \dots, n \quad (1)$$

between the reference and each template image $\{S_i\}_{2 \leq i \leq n}$. The considered mappings f depend crucial on the monitored direction of the reference image S_1 . E.g., let S_1 be recorded in frontal, S_2 in sagittal and S_2 in horizontal direction, then the affine linear mappings are restricted to the form

$$f^{(i)}(A, b)(x) = \underbrace{M_1 \circ R \circ M_2}_{=:A} x + b = Ax + b \quad (2)$$

where R is the rotation matrix according to the three axis (e.g., see [4]), b is the translation vector and

$$M_1 := \begin{pmatrix} 1 & 0 & 0 \\ 0 & s_2 & 0 \\ 0 & 0 & s_3 \end{pmatrix} \quad \text{resp.} \quad M_2 := \begin{pmatrix} s_1 & 0 & 0 \\ 0 & 1 & 0 \\ 0 & 0 & 1 \end{pmatrix} \quad (3)$$

are scaling matrices. We combine the searched parameters to a vector $m = (s_1, s_2, s_3, r_1, r_2, r_3, b_1, b_2, b_3)^T$. This leads us to a nine-dimensional minimization problem $\min_m g(m)$ for each pair of images. To solve the optimization problem several approaches are proposed in the literature, e.g. the authors in [2,5] use the Powell-algorithm, in [7] the Downhill-algorithm, the minimization approach in [1,6] is based on a singular value decomposition and the Levenberg-Marquardt iteration is used in [3]. Due to the fact that in our application the condition of the resulting Jacobian is small, the resulting minimization problem is solved just by a Gauss-Newton iteration with additional line-search. Therefore we determine a descend direction

$$d = \operatorname{argmin}_{\Delta m} \{ \|B \Delta m - r\| \} \quad (4)$$

with $h(x) = S_1(x) - S_i(f_i(x))$ and $x_{i,j,l}$ the Jacobian is defined by

$$B = \begin{pmatrix} \frac{\delta h(x_{1,1,1}, m)}{\delta m_1} & \dots & \frac{\delta h(x_{1,1,1}, m)}{\delta m_9} \\ \vdots & \ddots & \vdots \\ \frac{\delta h(x_{n,m,l}, m)}{\delta m_1} & \dots & \frac{\delta h(x_{n,m,l}, m)}{\delta m_9} \end{pmatrix} \quad \text{and} \quad r = \begin{pmatrix} h(x_{1,1,1}, m) \\ \vdots \\ h(x_{n,m,l}, m) \end{pmatrix}, \quad (5)$$

by solving it's normal-equations $B^T B \Delta m = B^T r$. The reason is that this way we just have to do a 9×9 Cholesky-composition. A QR decomposition is unnecessary since the condition of this problem is acceptable small. B can be calculated either by a analytical differentiation or difference quotients. Of course there is no big difference between this possibilities, except the analytical differentiation leads to better results for small steps. The solution Δm is used in the line-search

$$\lambda^* = \arg \min_{\lambda > 0} g(m + \lambda \Delta m) \quad (6)$$

as direction. For a fast minimization of the functionals (1) a multiresolution framework is developed. Therefore the problem is solved in lower resolutions first. As lower resolutions the images are restricted to half the size in each direction until a fixed image resolution is achieved. The minimization problem is solved first on the coarsest resolution, by using initial guess which includes no rotation, the DICOM-scalings and a translation that centers the images according to each other. The resulting solution vector is adapted to the next finer resolution and is used there as initial guess. This is done until the finest resolution is reached. In the second step of the image fusion process the images are fused to an image I , which contains all features of the source images $\{S_i\}_{1 \leq i \leq n}$. Therefore, we use just a trilinear interpolation for the voxels $\{S_i(f_i(x))\}_{2 \leq i \leq n}$ and the fused image I is determined by

$$I(x) = \frac{S_1(x) + \sum_{i=2}^n S_i(f_i(x))}{n}. \quad (7)$$

3 Discussion

The function f has to fulfill different conditions. It should allow translation, rotations and a global scaling as well as taking care of that each image has one direction with lower resolution. The last condition is the reason why the scaling M is split in (1). As the images are matched to the frontal, the frontal scaling has to be done before the rotation, while the sagittal and horizontal scaling has to be done after the rotation. This allows also the global scaling for small angles. As the angles have to be small one restriction is that the images must have the same orientation. Another restriction is, that so far the slides must be equidistant. Instead of extending the images in some way, we just leave out any calculation in th sum, that would use values that would be outside the boundary. This speeds up the convergence significantly, as no "fake" boundary falsifies the descent direction. It also allows the images to be slightly different in what they show. But this assumes our start value is good enough to find not only a local but a global minimum.

4 Results

The shown results in Figure 2 which is a central slide of a fused 3D-image is quite what we tried to accomplish. The image is smooth and the artefacts of

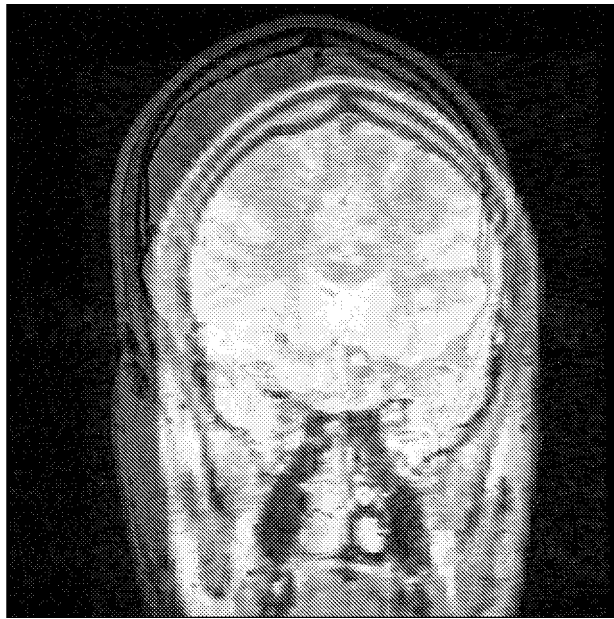


Fig. 1. The central slides of the unmatched frontal and sagittal image sets.

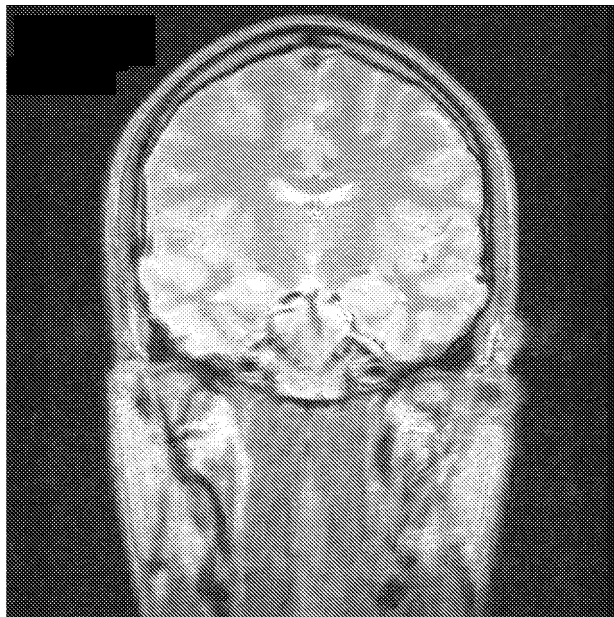


Fig. 2. . Central slide of the fused image.

the different resolutions are neglectable. In Figure 1 you see a slide of a given problem. The frontal image shown dark and the sagittal shown in white. One can notice the different resolutions of the images. Shown from this direction the frontal resolutions are high, while the sagittal has a low horizontal resolution. One can also notice that the sagittal image slide is not matching in any way to the frontal as we have a 3D-problem. In Figure 1 one can see the same frontal, but a different sagittal slide.

References

1. ARUN K.S., HUANG T.S. AND BLOSTEIN S.D., Least square fitting of two 3-D point sets, *IEEE Trans PAMI*, 9(5), pp. 698–700, 1987.
2. HATA N., SUZUKI M., DOHI T., ISEKI H., TAKAKURA K. UND HASHIMOTO D., Registration of ultrasound echography for intraoperative use: A newly developed multiproperty method, *Proc SPIE*, Vol 2359, Visualization in Biomedical Computing, SPIE Press, Bellingham, WA, pp. 251–259, 1994.
3. HAMADEH A., LAVALLEE S., SZELISKI R., CINQUIN P. UND PERIA O., Anatomy-based registration for computer-integrated surgery, *Lecture Notes in Computer Science*, Vol 905, Computer Vision, Virtual Reality and Robotics in Medicine, pp. 213–218, 1995.
4. H. HANDELS, *Medizinische Bildverarbeitung*, Teubner Verlag.
5. PELIZZARI C.A., CHEN G.T.Y., SPELBRING D.R., WEICHELBAUM R.R. AND CHEN C.-T., Accurate three-dimensional registration of CT, PET and/or MR images of the brain, *Journal Comput. Assist. Tomogr.*, 13(1), pp. 20–26, 1989.
6. UMEYAMA S., Least-squares estimation of transformation parameters between two point patterns, *IEEE PAMI* 13(4), pp. 276–380, 1991.
7. Mangin J.F., Frouin V., Bloch I., Bendriem B. und Lopez-Krahe J., Fast nonsupervised 3D registration of PET and MR images of the brain, *Journal of Cerebral Blood Flow and Metabolism*, 14, pp. 749–62, 1995.